

## mTOR is a promising therapeutical target in a subpopulation of pancreatic adenocarcinoma



Wesley K. Utomo<sup>a,1</sup>, Vilvapathy Narayanan<sup>a,1</sup>, Katharina Biermann<sup>b</sup>, Casper H.J. van Eijck<sup>c</sup>, Marco J. Bruno<sup>a</sup>, Maikel P. Peppelenbosch<sup>a,\*</sup>, Henri Braat<sup>a</sup>

<sup>a</sup> Department of Gastroenterology and Hepatology, Erasmus MC, Rotterdam, The Netherlands

<sup>b</sup> Department of Pathology, Erasmus MC, Rotterdam, The Netherlands

<sup>c</sup> Department of Surgery, Erasmus MC, Rotterdam, The Netherlands

### ARTICLE INFO

#### Article history:

Received 5 September 2013

Received in revised form 17 January 2014

Accepted 20 January 2014

#### Keywords:

Pancreatic cancer  
Personalized medicine  
mTOR  
Rapamycin  
Flow cytometry

### ABSTRACT

Pancreatic ductal adenocarcinoma (PDAC) remains a highly lethal disease, unusually resistant against therapy. It is generally felt that stratification of patients for personalized medicine is the way forward. Here, we report that a subpopulation of PDACs shows strong activation of the mTOR signaling cassette. Moreover, we show that inhibition of mTOR in pancreatic cancer cell lines showing high levels of mTOR signaling is associated with cancer cell death. Finally, we show using fine needle biopsies the existence of a subpopulation of PDAC patients with high activation of the mTOR signaling cassette and provide evidence that inhibition of mTOR might be clinically useful for this group. Thus, our results define an unrecognized subpopulation of PDACs, characterized by high activation of mTOR and show that identification of this specific patient group in the early phase of diagnosis is feasible.

© 2014 The Authors. Published by Elsevier Ireland Ltd. Open access under [CC BY-NC-SA license](http://creativecommons.org/licenses/by-nc-sa/4.0/).

### 1. Introduction

Pancreatic ductal adenocarcinoma (PDAC) is the 4th leading cause of cancer related death in the world and more than 260,000 people die of this disease every year worldwide [1]. Due to local invasion of vasculature or distant metastasis, only 15–20% of patients are surgical candidates at presentation. Of those operated, the 5-year survival is only 10–15% and adjuvant therapy only improves disease free survival from 5.5% to 16.5% at 5 years but has no impact on survival [2]. The median survival after diagnosis of locally advanced unresectable disease is 4–6 months, and 2–4 months for patients presenting with metastatic disease [3,4]. PDAC is among the most chemoresistant cancers and advancements in traditional chemotherapeutics have been especially disappointing as many targeted therapies have failed to show any benefit. Current palliative therapy is limited to patients with optimal performance score

(WHO 0–1) with only 4 months survival benefit in patients with metastatic disease (FOLFIRINOX) [5]. Research efforts are focused on early detection, and multimodality treatment with surgery and chemoradiation. Personalized medicine-based therapy might be another approach to achieve significant long term benefit in patients with PDAC [6].

PDAC is a heterogeneous disease with different pathways affected in different patients. Next generation sequencing and microarray analysis have revealed a set of 12 core cellular signaling pathways and processes that were genetically altered in 67–100% of PDAC tumors. These genetic alterations involve pathways such as apoptosis, KRAS, Hedgehog, WNT/Notch, TGF-beta, and DNA repair pathways [7]. Mutations in the KRAS gene along with activation of EGFR and loss of telomeres are required for the initiation of PDAC [8–10]. The progression of PDAC requires the constitutive activation of Ras/mammalian target of Rapamycin (mTOR) or Ras/MEK/ERK pathways [11–13]. In PDAC, levels of phospho S6 (pS6), the activated form of a downstream protein of the mTOR pathway involved in translation initiation, are markedly increased [14–16]. Moreover, mTOR pathway activation is shown in pancreatic cancer cell lines, tumor xenografts, human pancreatic tumors, and in a number of other human tumors [17–19]. Previous studies have shown mTOR pathway activation in PDACs, approximated between 25% and 75% [14,19]. The mTOR pathway consists of two protein complexes, in which mTOR, raptor and mLST8 proteins constitute to form the mTOR Complex 1 (mTORC1) and mTOR, rictor and

\* Corresponding author. Address: Department of Gastroenterology and Hepatology, Erasmus MC, room NA-1007, 's Gravendijkwal 230, NL-3015 CE Rotterdam, The Netherlands. Tel.: +31(0)107032792; fax: +31 (0)107032793.

E-mail address: [m.peppelenbosch@erasmusmc.nl](mailto:m.peppelenbosch@erasmusmc.nl) (M.P. Peppelenbosch).

<sup>1</sup> These authors contributed equally to this work.

Sin1 proteins forming mTOR complex 2 (mTORC2). In cellular growth and associated proliferation, mTORC1 plays a vital role by integrating signals from nutrients and energy status. It regulates several processes like ribosome biogenesis, protein synthesis, metabolism and autophagy [20]. mTORC2 plays a role in cytoskeletal organization through protein kinase C and paxillin [21]. Rapamycin, and its synthetic derivatives (rapalogs), can inhibit the mTOR pathway by binding to FK-binding protein-12, which in turn binds to the mTOR protein, and subsequently preventing the assembly of mTORC1 [22]. Prolonged use of rapalogs has shown to disrupt mTORC2 as well [23]. Several clinical trials involving rapalogs showed clinical benefit in only a minority of pancreatic cancer patients, however none of the studies involved a sensitivity assay of the tumor to rapamycin or rapalogs [17,24]. In view of the molecular heterogeneity of PDAC, the activity of the Ras/mTOR pathway, and incidental benefit of rapalog treatment in PDAC, we hypothesize that a subpopulation of PDAC patients sensitive for rapalog treatment could be identified using *ex vivo* biopsies. Hence, the mTOR axis can be a promising target to be included in treatment protocols for PDAC using rapamycin or rapalogs in a subpopulation of patients.

## 2. Material and methods

### 2.1. Cell lines

Pancreatic cancer cell lines BxPC3, Su86.86, HPAF, and HS700T were cultured as confluent monolayers in RPMI-1640 (Gibco) with penicillin and streptomycin (Invitrogen) and 7.5% Fetal Calf Serum (FCS) (Sigma–Aldrich) using routine procedures (5% CO<sub>2</sub>, at 37 °C). Capan-1 was cultured using IMDM (Gibco) supplemented with 20% FCS. The cell lines were a kind gift of the department of surgery of the Erasmus MC. The cell lines were authenticated by means of a STR-analysis.

### 2.2. Patients and specimens

Appropriate ethical approval was obtained for all procedures involving patients or patient material. We included 64 slides of 39 formalin fixed paraffin embedded (FFPE) specimens from pancreatic surgery with a histologically confirmed PDAC or neuroendocrine tumor. The tissue blocks were collected from a prospectively maintained pathology tissue bank at the Erasmus MC. Specimens were sectioned at 5 µm (Microm HM325 Microtome), incubated at 37 °C overnight, and stored until used for immunohistochemistry staining.

Endoscopic ultrasound guided fine needle aspiration biopsies (EUS-FNABs) were obtained from patients suspected for pancreatic cancer (or with a pancreatic mass lesion). All patients provided written informed consent. The EUS-FNABs were obtained from the endoscopy department and transported to the laboratory in RPMI-1640 medium with 10% FCS. The biopsy was washed three times with PBS containing penicillin and streptomycin (Invitrogen). Single cell suspensions were prepared using 0.5 mg/ml collagenase IV (Sigma–Aldrich) and pushed through a 100 µm cell strainer (BD Falcon). The cells were suspended in RPMI-1640 (Gibco) and counted using a slide with counting grids (Kova Glasstic® Slide 10, Hycor Biomedical Ltd., Penicuik, UK).

### 2.3. Immunohistochemistry

Tissue sections were deparaffinized in xylene for 5 min and rehydrated using ethanol. The endogenous peroxidase activity was blocked with methanol and 3% H<sub>2</sub>O<sub>2</sub> followed by tap water immersion for 5 min. Antigen retrieval was performed by boiling in preheated buffer 10 mM citrate buffer pH 7.6 for 10 min at 200 W in a microwave. Next, slides were blocked by 10% goat serum in phosphate-buffered saline tween pH 7.4 for 1 h at room temperature. Primary antibodies rabbit monoclonal anti-pS6 (1:250, Cell Signaling Technology, Beverly, MA, USA) was added and incubated at 4 °C overnight. Envision goat anti-rabbit-horseradish peroxidase (DAKO, Denmark) was used as secondary antibody [25]. WKU and VN scored the slides independently in a blinded manner. Five high power fields were counted for each slide. The percentage of cells that stained positive (immunoreactivity above background) in the area was quantified. The pS6 level was scored as follows: a score of 0 for less than 3%, a score of 1 between 3% and 10%, a score of 2 between 10% and 50%, and a score of 3 for more than 50% of positively stained cells (scoring system developed by KB). Pictures were taken using the Zeiss Axioskop20 microscope, Nikon Digital Sight DS-U1 camera and NIS-Elements 3.00 program.

### 2.4. Cell viability assay

To assess the effect of rapamycin on pancreatic cancer cell lines we used a MTT-assay. In short, 10,000 cells from each cell line were incubated with 3-(4,5-dimethylthiazol-2-yl)-2,5-diphenyltetrazolium bromide (MTT). The purple formazan is measured at 490 nm and 595 nm using a microplate reader (Model 680XR Bio-Rad) at 72 h. The functional viability of cells was calculated using the mean OD in sample well divided by the mean OD in the control well × 100%. To show the correlation of increasing concentration of rapamycin with cytotoxicity in pancreatic cancer, we used a linear regression to reject the null hypothesis where changes in rapamycin concentration are not associated with increased cell death. The *p*-value is considered significant when *p* < 0.01.

### 2.5. Western blot

Western blotting was performed according to standard fluorescent Odyssey immunoblotting (Li-COR Biosciences, Lincoln, NE, USA). Antibodies specific for pS6 and light chain 3 (LC3A/B-I and II) (all 1:1000, Cell Signaling Technology) were used. To ascertain equal loading and normalization of the protein for quantification, beta-actin (1:2000, Santa Cruz) was used. The secondary antibodies used for detection were goat anti-rabbit and rabbit anti-mouse (1:5000, Li-COR Biosciences). Transfer membranes were transferred to 50 ml sterile light-protecting centrifuge tubes (Greiner bio-one), incubated with secondary antibodies and washed. Fluorescence Odyssey system (Li-COR Biosciences, Lincoln, NE, USA) was used to visualize and quantify protein expression. Semi quantitative expression data were determined by Odyssey 3.0 software and normalized using beta-actin for reference gene protein expression [25].

### 2.6. Flow cytometry

To assess pS6 expression levels, we analyzed pancreatic cancer cell lines and single cell suspensions prepared from EUS-FNABs as described above, using flow cytometry.

The pancreatic cancer cell lines were washed with 0.1% sodium chloride (Sigma–Aldrich) in PBS and trypsinized with 0.05% trypsin EDTA (Invitrogen). A minimum of 100,000 cells were used for each assay. The cells were divided in the following three conditions during 2 h: blank unstained cells, RPMI-1640 only (to measure basal pS6 levels), and RPMI-1640 with 0.1 µM rapamycin (to measure inhibition of pS6). The same conditions were applied to single cell suspensions from EUS-FNABs.

Cell permeabilisation was done with a permeabilisation buffer (0.5% saponine, 1% FCS, 0.02% EDTA in PBS). The cells were stained using cytokeratin 8/18 mouse mAb (CK8/18; 1:100; Cell Signaling Technology) and secondary labeled with anti-Mouse IgG eFluor® 660 (1:100; eBioscience, Ltd., UK) to mark epithelial cells. CK8/18 has been shown to be expressed as much as 100% in PDAC [26]. Finally, we stained the samples with V450 Mouse anti-pS6 (1:50; BD Biosciences, Breda, Netherlands). Data was analyzed using FlowJo (v 7.6.5, Treestar, Ashland, OR). Mean Fluorescence Intensity (MFI) was calculated using the geometric mean of the CK8/18+population. Mean values were compared using a student *T*-test.

## 3. Results

### 3.1. A subpopulation of PDACs is characterized by strong activation of the mTOR signaling cassette

To study activation of the mTOR pathway in pancreatic cancer, we performed an immunohistochemical staining of a set of FFPE specimens that contains 42 normal acinar regions, 42 normal ductal epithelium, 15 PanIN lesions, 7 neuroendocrine tumors, and 39 PDAC regions for the levels of pS6 (Fig. 1). The proportion of tissue expressing pS6 is 50% in normal ducts, 67% in PanIN lesions, and 82% in adenocarcinoma regions (Fig. 1). Normal acinar regions show high levels of pS6, while normal duct epithelium exhibits much lower pS6 levels overall (Fig. 2A). Since it has been shown that the mTOR pathway is deregulated in neuroendocrine tumors (NET), we used NETs as positive controls [27] (Fig. 2B). Differences in pS6 staining were observed between various patients with PDAC, especially differential staining of dysplastic ducts and stroma can be pronounced (compare Fig. 2C with Fig. 2D). The variability in pS6 levels was also seen in various PanIN lesions (Supplementary Figs. S1A and S1B). Thus, substantial variation in the activation of mTOR pathway exists and our results demonstrate the presence of a subgroup of pancreatic adenocarcinoma

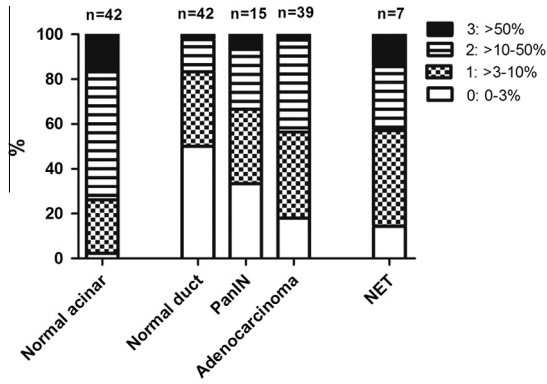
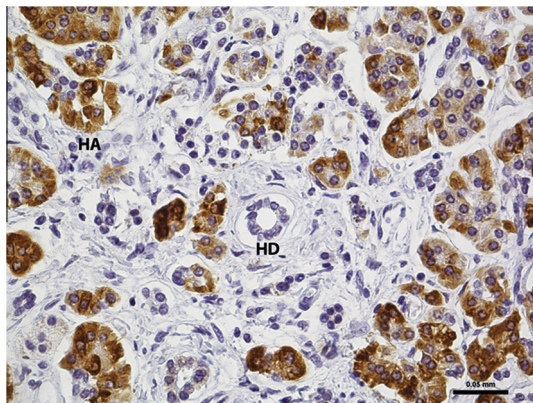
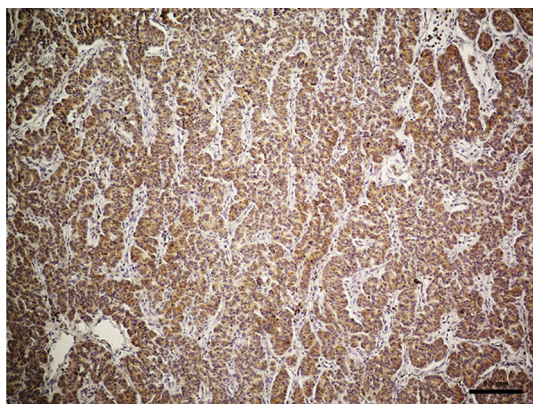


**Fig. 1.** Graph presenting proportion of pS6 levels in various histological conditions. Normal acinar regions were adjacent to PDAC regions. Normal duct represents the fraction of positive ductal epithelium in normal regions. PanIN lesions were also evaluated based on the positive staining of abnormal epithelium. The proportion of samples staining positive for pS6 increases from normal ductal epithelium to PDAC. NETs were used as positive control and had similar distribution to PDACs. The scoring system is described in the materials and methods section.



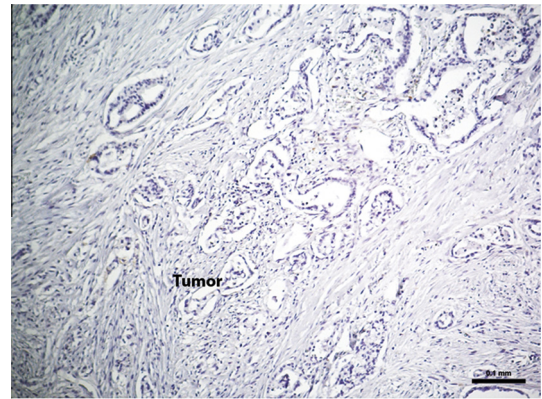
**Healthy region**

**Fig. 2A.** Representative normal region adjacent of PDAC stained for pS6. Normal duct epithelium (HD) score 0, which was found in 50% of the cases. Normal acinar region (HA) score 3 (20×).



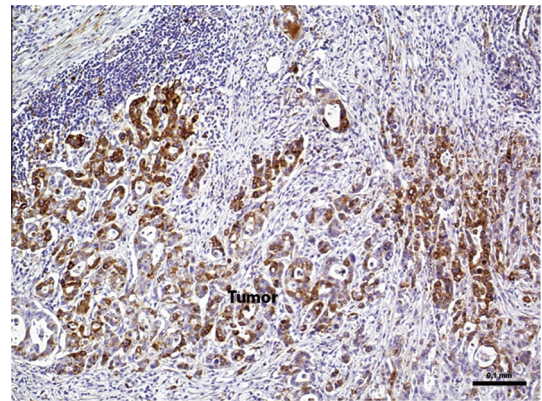
**Neuroendocrine tumor**

**Fig. 2B.** Representative image of a pancreatic neuroendocrine tumor (NET), score 3 (10×). NETs were stained as positive controls as it has been shown that activation of the mTOR pathway, mediated by IGF-1, is necessary for proliferation in pancreatic NETs [45].



**Tumor region score 0**

**Fig. 2C.** Representative adenocarcinoma region, score 0 (10×). Staining less than 3% of the adenocarcinoma was observed.



**Tumor region score 3**

**Fig. 2D.** Representative adenocarcinoma region, score 3 (10×).

that is characterized by very strong activation of the mTOR signaling cassette.

**3.2. Rapamycin-dependent cytotoxicity in pancreatic cancer cell lines correlates with the level of mTOR-dependent signaling**

A logical question arising from our discovery of a mTOR hyperactivated subset of PDAC is whether cancer survival is dependent on activation of this signaling cassette in such cancers. To this end, we compared pancreatic cancer cell lines exhibiting different levels of mTOR activation for their sensitivity to the mTOR inhibitor. We determined pS6 levels in BxPC3, Su86.86, HS700T, HPAF, and Capan-1 and its inhibition after 2, 6, and 18 h incubation with 0.1 μM rapamycin. BxPC3 and SU86.86 are most sensitive to rapamycin with a decrease of pS6 expression up to 655 and 355-fold ( $p < 0.01$ ) in Western blot respectively (Fig. 3), and thus, display most mTOR signaling activity. Rapamycin induced decrease of pS6 expression was less pronounced in Capan-1, HPAF, and HS700T cells, with up to a 10-fold decrease after 2 h (Fig. 3), and therefore, these cell lines are characterized by a substantial lower degree of rapamycin sensitivity. The level of rapamycin-sensitive mTOR activity correlated well with the cytotoxic effects of rapamycin. In BxPC3 (Fig. 4A) and SU86.86 (Fig. 4B) 12.5 nM rapamycin decreases cell viability to 69% (±10.0%) and 75% (±4.0%), respectively. In contrast, HS700T, HPAF, and Capan-1 pancreatic cancer cells show much less pronounced mTOR activation. Accordingly,

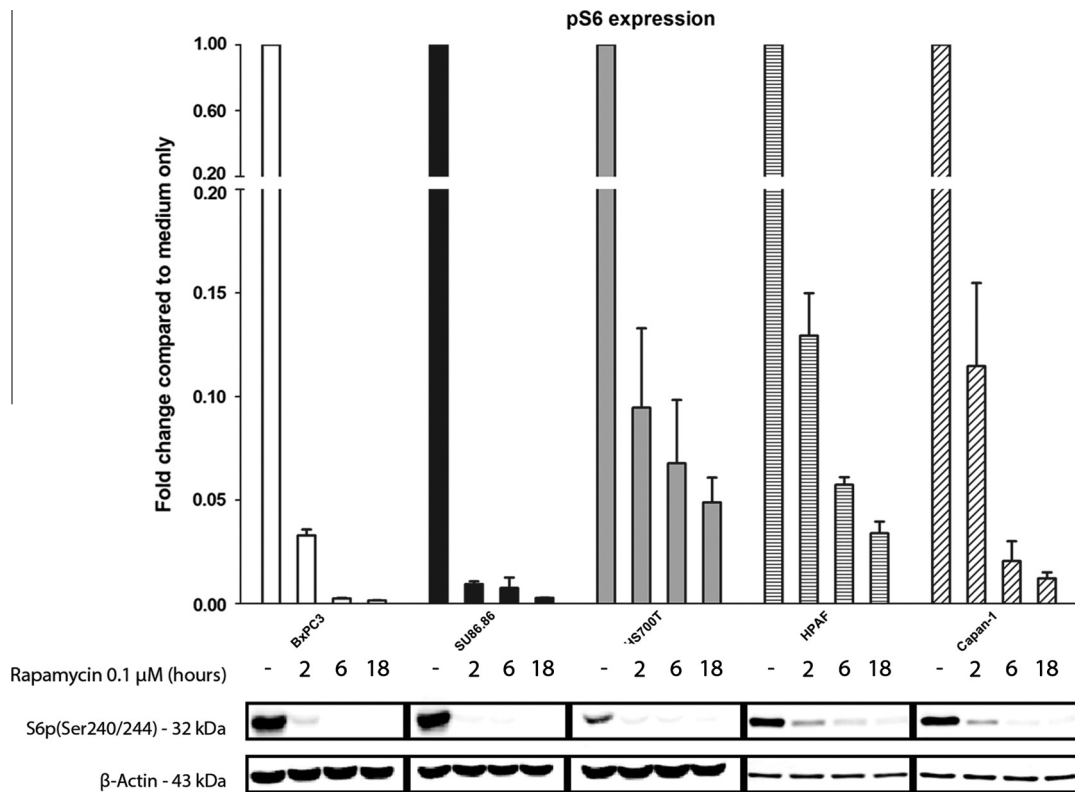


**Fig. 3.** Western blot analysis and quantification of phosphorylated S6 in BxPC3, SU86.86, HS700T, HPAF, and Capan-1. The cell lines were exposed to increasing duration of 0.1  $\mu$ M rapamycin. Lysates were subjected to pS6 antibodies and subsequently quantified and normalized against beta-actin. Higher basal expression of pS6 is seen in BxPC3 and SU86.86 compared to HS700T. In BxPC3, rapamycin inhibits phosphorylation of S6 by 30, 392, and 655-fold after 2, 6, and 18 h respectively with rapamycin. Similarly, in SU86.86 this effect is 106, 132, and 355-fold in the same conditions. HS700T is less rapamycin-sensitive as seen by a less pronounced decrease of pS6 expression (11, 15, and 20-fold decrease). The inhibition of pS6 levels in HPAF and Capan-1 were also lower, exhibiting a 8, 17, and 29-fold decrease in HPAF, and a 8, 48, 82-fold decrease in Capan-1. Experiment was performed in duplicate, one representative blot is shown.

Capan-1 (Fig. 4C) and HPAF (Fig. 4D) show no response to rapamycin, exhibiting cell viabilities of 113.4%( $\pm$ 6.0%) and 131.4%( $\pm$ 18.4%) at 200 nM concentration. HS700T cells shows 80.8%( $\pm$ 1.9%) cell viability in the presence of 12.5 nM rapamycin and more than 50 nM rapamycin is needed to obtain a comparable decrease in cell viability as in BxPC3 cells (Fig. 4E). Thus, high activation of mTOR shows a correlation with increased sensitivity to mTOR inhibition in pancreatic cancer. To illustrate the correlation between pS6 inhibition and cell viability we plotted both parameters for all cell lines. The mean pS6 inhibition after 2 h incubation with 0.1  $\mu$ M rapamycin of both responsive and non-responsive cell lines (derived from western blot) was plotted against the percentage of cell viability as measured by MTT-assay with the same concentration of rapamycin (Fig. 5). Sensitivity to mTOR inhibition is correlated with decreased cell viability for the rapamycin responsive cell lines but not for the rapamycin unresponsive cell lines.

### 3.3. Rapamycin induces autophagy in rapamycin sensitive pancreatic cancer cell lines

Subsequently, we were interested in the molecular mechanism of cytotoxicity in mTOR-proficient pancreatic cancer cell lines. In the canonical response to rapamycin, induction of autophagy and apoptosis are considered the major effectors here. To assess the role of autophagy and apoptosis in rapamycin induced decrease of cell viability of pancreatic cancer cell lines, we performed Western blot analysis on LC3A/B-I and II. The expression of LC3A/B-II increased 2.4-fold in both BxPC3 and SU86.86, after 18 h incubation with rapamycin (Fig. 6). In contrast to BxPC3 and SU86.86, we did not observe a significant increase of LC3A/B-II in HS700T,

HPAF, or Capan-1 (Fig. 6). These results support a role for hyperactivated mTOR for maintaining survival in a subpopulation of PDAC.

### 3.4. Sensitivity to rapamycin in pancreatic cancer cell lines can be measured using flow cytometry

We have shown in Western blot that rapamycin reduces phosphorylation of S6 in pancreatic cancer cell lines. To translate this into an *ex vivo* sensitivity assay, to a protocol useful for personalized medicine in clinical practice, we measured phosphorylation of S6 in pancreatic cancer cell lines using flow cytometry. Rapamycin resulted in an absolute reduction of CK 8/18+pS6+cells by more than 40% in BxPC3 (Fig. 7A) and SU86.86 (Supplementary Fig. S2). In contrast, there was a minimal reduction of less than 1% within the CK8/18+pS6+population in the rapamycin-unresponsive cell lines; HS700T (Fig. 7B), Capan-1 (Supplementary Fig. S3A), and HPAF (Supplementary Fig. S3B). We observed the same effect of rapamycin on the amount of pS6 per cell as shown in Fig. 7C. Thus, flow cytometry is in principle useful for determining the sensitivity of pancreatic cancer cells to mTOR inhibition.

### 3.5. The mTOR pathway is activated in a subfraction of EUS-FNABs from pancreatic cancer patients and is potently inhibited by rapamycin

Finally, we determined *ex vivo* mTOR pathway activation in biopsies obtained through endoscopic ultrasonography in patients suspected for pancreatic cancer. Two hours of incubation with 0.1  $\mu$ M rapamycin inhibited pS6 levels in CK8/18+cells in two out of nine samples (22%). In those two samples we identified as

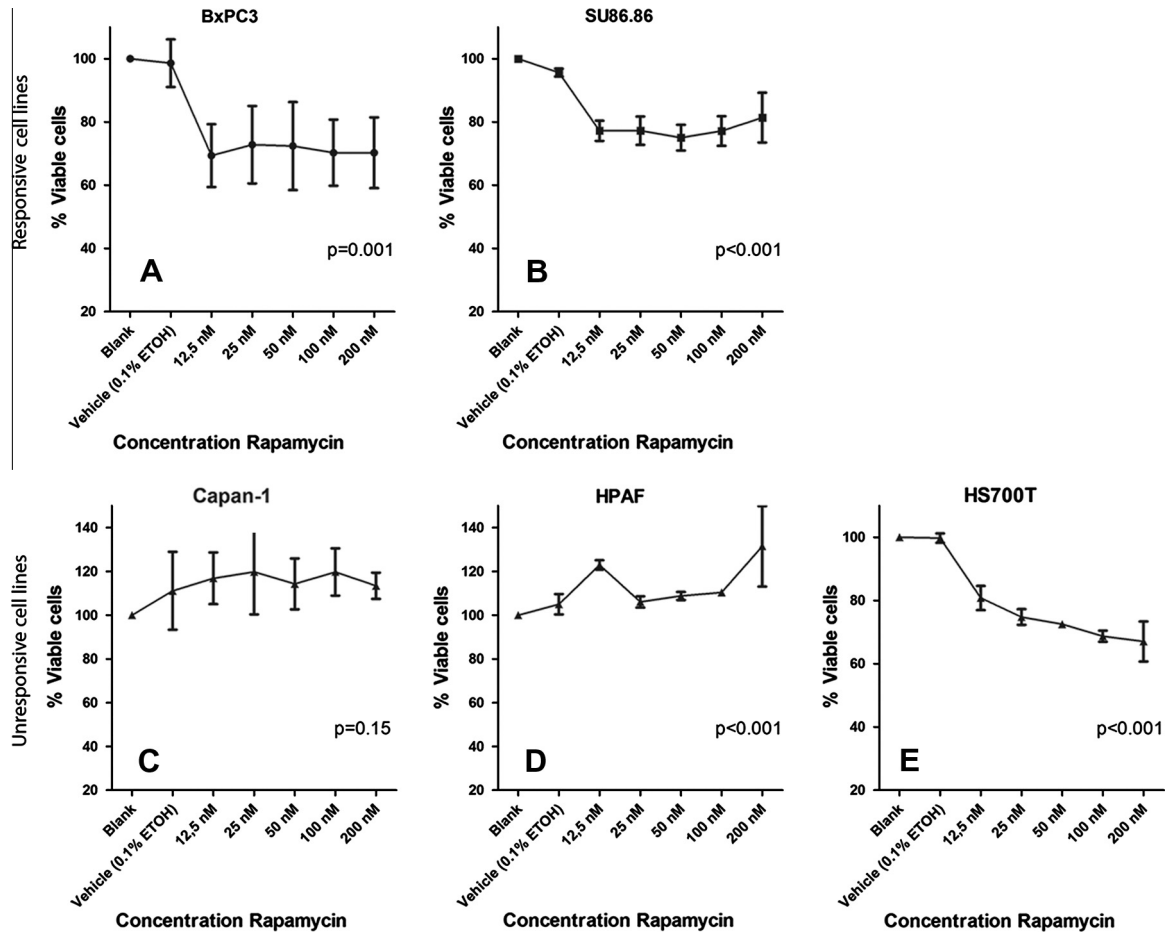


**Fig. 4.** Graphs depicting the effect of rapamycin on cell viability in pancreatic cancer cell lines. BxPC3 (A), SU86.86 (B), Capan-1 (C), HPAF (D), and HS700T (E) were treated with increasing doses of rapamycin for 72 h. Mean values are averages from 3 independent experiments performed in triplicate.

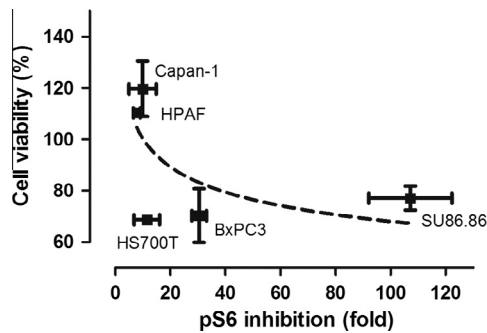


**Fig. 5.** Scatter plot showing the correlation of pS6 levels and predicted cytotoxicity. On the x-axis is the fold pS6 inhibition (retrieved from western blot with 2 h 0.1  $\mu$ M rapamycin) and cell viability on the y-axis (retrieved from MTT-assay with 0.1  $\mu$ M rapamycin). A non-linear regression curve was fitted through the available datapoints indicating that higher inhibition of pS6 levels correlate with higher rapamycin-dependent cytotoxicity. Responsive cell lines (BxPC3 and SU86.86) are in the higher range of pS6 inhibition, corresponding with lower cell viabilities. In contrast, lower pS6 inhibition in cell lines correspond to better survival of pancreatic cancer cells (Capan-1 and HPAF). HS700T however, exhibit declining cell viability without proper mTOR inhibition, most likely due to off-target effects.

'potential responders', rapamycin led to a relative reduction of more than 90% (94.2% and 98.4%) in the amount of pS6 expressing cells. Fig. 8 depicts two representative scatter plots and histograms of a patient with high levels of pS6 and response to rapamycin treatment (Fig. 8A) and a patient with no response to rapamycin

(Fig. 8B). To measure the phosphorylation of S6 per cell, the pS6 MFI of CK8/18+ cells was calculated. Potential responders ( $n = 2$ ) showed a mean reduction in MFI of 81.3% ( $\pm 2.7\%$ ), while the average MFI change in non-responders ( $n = 7$ ) was 8.8% ( $\pm 6.1\%$ ) ( $p < 0.01$ ) (Fig. 8C). Thus, EUS-FNAB and flow cytometry are useful for identifying potential responders to rapamycin therapy.

**4. Discussion**

Our *ex vivo* analysis on EUS guided FNABs of patients shows that 22% of PDAC patients potentially benefits from treatment with rapalogs. This number is in accordance to what was observed in a pre-clinical setting in mice, where rapamycin induced regression in 4 out of 17 xenografts (23.5%) [14]. However, the presence of feedback loops after mTOR inhibition can induce therapy resistance in these patients [28]. Consequently, the question remains whether these patients can be treated with rapalog monotherapy or whether rapalog will be part of a treatment protocol. In the coming years it will become clear whether strategies involving combination therapy with second generation mTOR inhibitors which inhibit mTORC1 and mTORC2 [29], dual mTOR/PI3K inhibitors which block the PI3K/Akt feedback activation [30], or the addition of JAK2/STAT5 inhibitors [31] will prove beneficial in PDAC.

Pancreatic cancer is a heterogeneous disease, with various different mutations in individual genes among a diversity of pathways [7]. The idea of tumor heterogeneity in pancreatic cancer is a concept that has been established decades ago [32]. In our immunohistochemistry data we confirmed heterogeneity in terms of

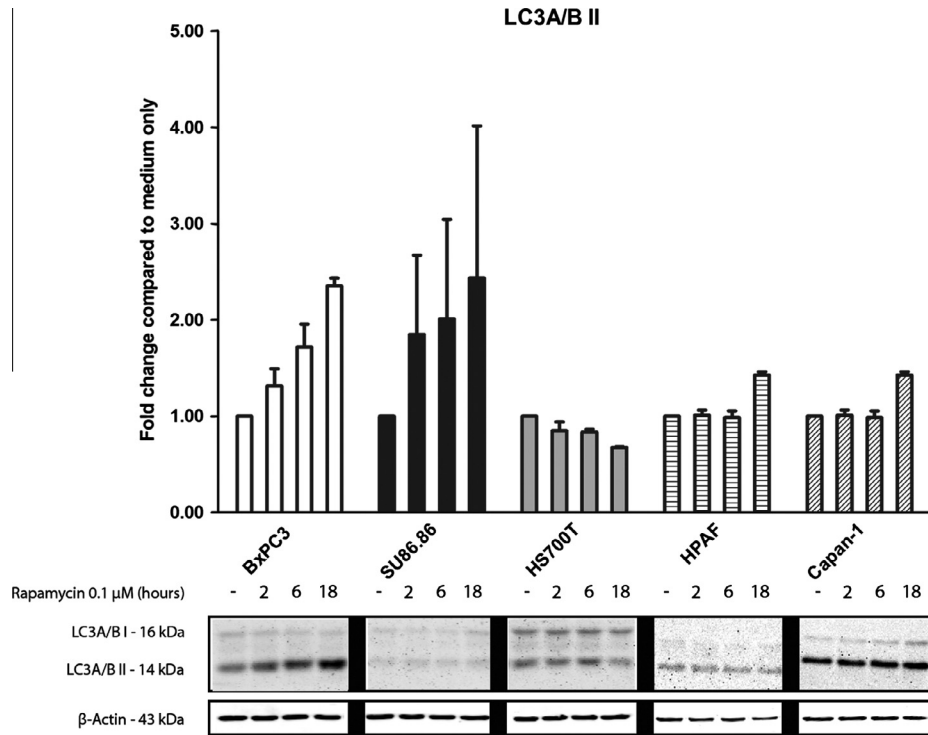


**Fig. 6.** Western blot analysis and quantification of autophagy marker LC3A/B in BxPC3, SU86.86, HS700T, HPAF, and Capan-1. The cell lines were treated with increasing duration of 0.1  $\mu$ M rapamycin. Next, we prepared lysates and these were subjected to LC3A/B antibodies. The expression of LC3A/B-II increases during prolonged incubation with rapamycin in rapamycin-sensitive cell lines. We quantified the expression of LC3A/B-II, normalized against beta-actin, as indicator of autophagy.

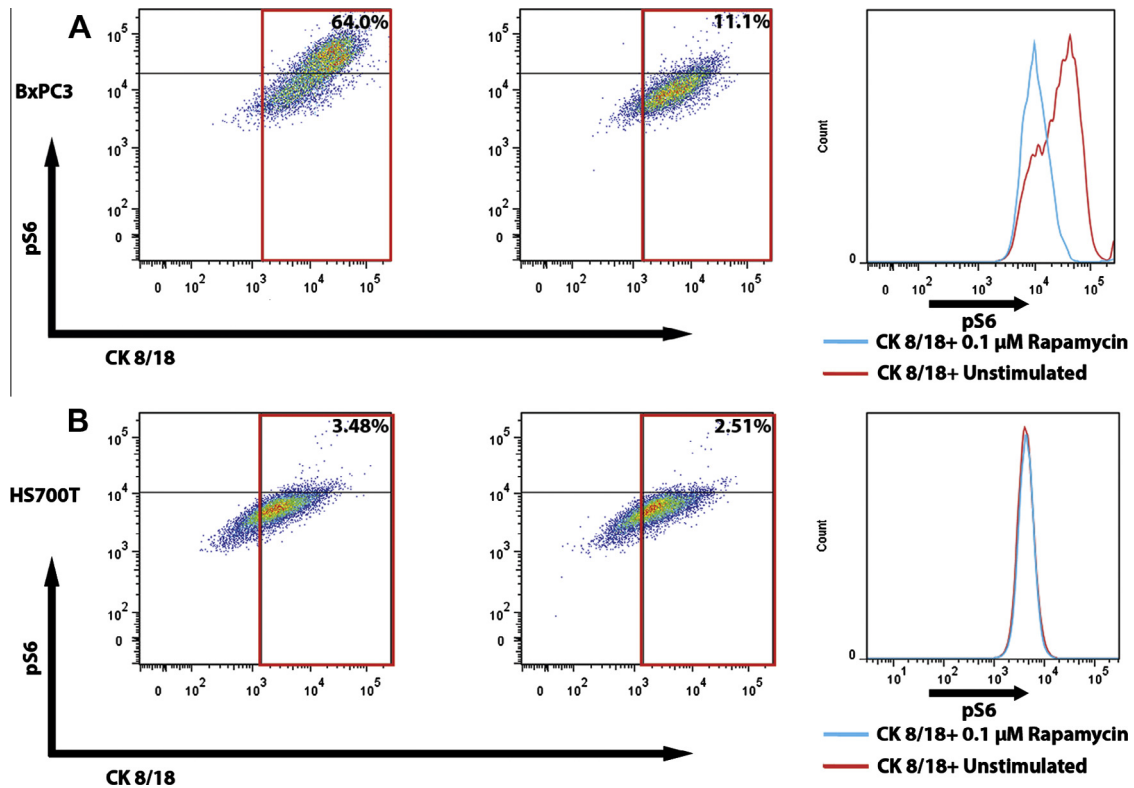


**Fig. 7.** Flow cytometry scatter plots and corresponding overlay histograms of a responsive cell line – BxPC3 (A) and a non-responsive cell line – HS700T (B). In accordance with our western blot data, BxPC3 display higher basal mTOR activation in the CK8/18+population (64.0%). This CK8/18+pS6+population was effectively reduced after 2 h incubation with 0.1  $\mu$ M rapamycin to 11.1%. In contrast, basal mTOR activation in HS700T was markedly lower (3.48%) and the effect of rapamycin on the CK8/18+pS6+population was therefore diminished. The overlay graphs are a representation of the count (y-axis), in the CK8/18+population (marked by the red box), within the pS6-channel (x-axis).

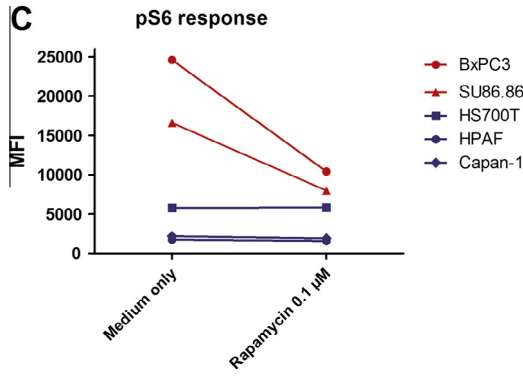


**Fig. 7C.** Graphical overview of the mean fluorescence intensity (MFI) of all cell lines incubated with and without 0.1 μM rapamycin during 2 h. The MFI change in rapamycin-sensitive cell lines was 57.7% and 51.9% for BxPC3 and SU86.86, respectively. In HS700T the change in MFI was 0.8%. Capan-1 and HPAF exhibited reductions of 9.8% and 13.0%, respectively. The MFI was calculated within the CK8/18+population only.

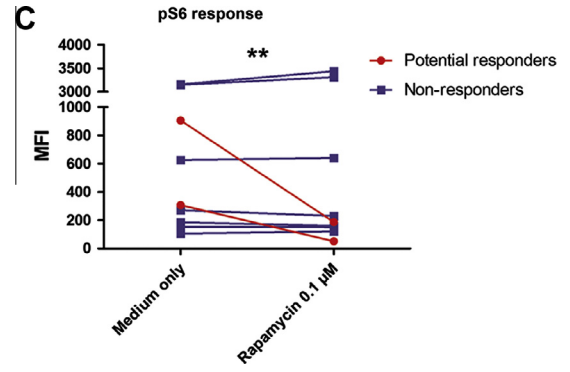


**Fig. 8C.** Graph depicting changes in MFI in potential responders and non-responders. Single cell suspensions from EUS-FNABs were measured using flow cytometry. Each sample was incubated without and with 0.1 μM rapamycin for 2 h. We selected the CK8/18+population and calculated the MFI in each condition. Two samples displayed a substantial reduction in MFI by an average of 81.3%. Seven samples were classified as non-responders due to the minimal change in MFI after treatment with rapamycin.

mTOR activation. During tumor genesis we observe a gradual increase in mTOR activation from normal ducts, to PanIN lesion, and finally in PDAC. This heterogeneity is also observed between PDACs, which makes selection of patients necessary to avoid futile treatment. Moreover, we also observed high mTOR activation in normal acinar region. However, the normal acinar regions were taken adjacent to adenocarcinoma so it is debatable whether morphological normal areas are actually normal, considering the yet unknown origin of PDAC [33].

The data from the western blot and MTT-assay show increased cytotoxicity in pancreatic cancer cell lines with hyperactivated

mTOR pathway after the addition of rapamycin. Both responsive cell lines (BxPC3 and SU86.86) show significant correlation of increasing dose of rapamycin with cytotoxicity ( $p \leq 0.001$ ). In comparison, unresponsive cell lines do not show a clear threshold effect but rather a dose response effect as can be observed in HS700T (most likely due to off-target effects). To further study the mechanism behind increased cytotoxicity, we analyzed autophagy (type 2 cell death) in our pancreatic cancer cell lines. Interestingly, we observed that rapamycin only induced autophagy in rapamycin sensitive pancreatic cancer cell lines. In contrast,

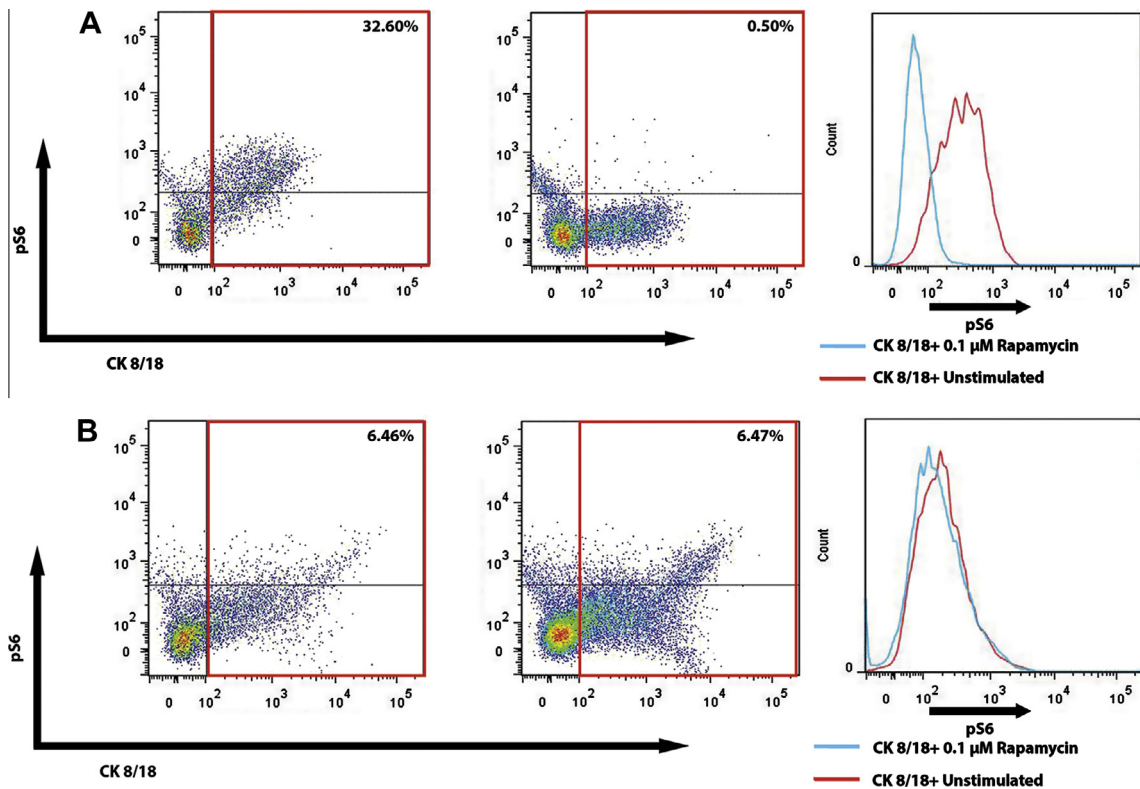


**Fig. 8.** Representative flow cytometry scatter plots and corresponding overlay histograms of a potential responder (A) and non-responder (B). The potential responder exhibited activation in the mTOR pathway which responded to rapamycin. The non-responder showed no change in the CK8/18+pS6+population after treatment with rapamycin. The overlay graphs are a representation of the count (y-axis), in the CK8/18+population (marked by the red box), within the pS6-channel (x-axis).

some pancreatic cancer cell lines (HPAF, Capan-1, and HS700T) seem insensitive to rapamycin, which is also reflected in a lower degree of pS6 inhibition and failure to induce autophagy. Rapamycin has been shown to induce autophagy pancreatic cancer cell lines before [34]. In this context however, autophagy was most likely activated due to the antitumor effect of rapamycin rather than a protective response [34,35]. Whether autophagy in cancer is a pro-survival process or part of antitumor effects is still point of discussion. Yang et al. found that in the case of pancreatic cancer, autophagy is needed for tumorigenic growth [36]. Therefore, they recommend trials in PDAC using drugs targeting autophagy, such as chloroquine.

Using flow cytometry, we show that the responsiveness of a tumor for rapamycin can be quantitatively assessed. Our pancreatic cancer cell line data indicate that hyperactivation of the mTOR pathway in PDAC can be potentially inhibited by tolerable concentrations of rapamycin. Hyperactivation of the mTOR pathway is also seen in patients with the Peutz-Jeghers syndrome where mutations in LKB1 can lead to inactivation of the LKB1/AMPK/TSC axis and thereby activating mTORC1, and eventually leading to the development of tumors [37]. Interestingly, 3–35% of PDACs have been shown to have loss of LKB1 expression in multiple studies [38,39] and most likely subsequent mTOR activation. To further support the rationale of the use of mTOR inhibitors, Klumpen et al. reported successful use of a rapalog (everolimus) in the treatment of a patient with advanced pancreatic cancer suffering from Peutz-Jeghers syndrome [40], supporting the need for individualized treatment. The question remains how to obtain tumor samples for stratification, and we believe EUS guided FNAB could be helpful in this situation. Phenotyping of these EUS-FNABs using flow cytometry shows that the determination of rapamycin sensitivity in clinical setting is possible, paving the way for personalized medicine.

Our study has some limitations pertaining the translation into an *in vivo* situation. We could not directly correlate our flow cytometry data of EUS-FNABs with immunohistochemical staining of the same samples due to insufficient material. Furthermore, in our sensitivity assays of EUS-FNABs, we did not include measurements of cell viability. Therefore, solely blocking the mTOR pathway in a patient might not be sufficient to combat the tumor, regardless of sensitivity towards rapamycin or rapalogs.

The results of our study suggest that it is possible to identify a subpopulation of pancreatic cancer patients with mTOR activation that are eligible for treatment with rapalogs. The lack of this test in previous studies with rapalogs might be an explanation for the disappointing results; only 20% would have been sensitive to rapalog treatment. Similarly, some pancreatic cancer cell lines seem totally resistant to mTOR inhibition, which may explain the failure of rapamycin therapy in unselected pancreatic cancer patients. Consistent with previous literature, we found an activation of the mTOR pathway in cell lines, resection specimens, and EUS-FNABs of PDAC [19,41]. This activation in pancreatic cancer cell lines and EUS-FNABs was effectively blocked by rapamycin in western blot and flow cytometry analysis. Furthermore, inhibition of pS6 levels by rapamycin are a good predictor of later cytotoxicity of the drug or its analogues. Targeting mTOR using rapalogs has recently shown to be efficacious in several neoplastic diseases such as pancreatic neuroendocrine tumors [42], hormone receptor positive breast cancer [43], and renal cell carcinoma after the failure of treatment with sunitinib or sorafenib [44].

We conclude that tumor tissue obtained in a minimal invasive way by means of endoscopic ultrasound guided fine-needle biopsy in chemotherapy naïve PDAC patients can be used *ex vivo* to identify a subpopulation of approximately 22% of patients that are potentially responsive to rapalog treatment. Such selection of patients for targeted treatment avoids futile treatment and

potentially improves the outcome of existing chemotherapeutic regimens. Given our findings, future research should aim for combining *ex vivo* drug sensitivity analysis using pS6 flow cytometry analysis as biomarker for therapeutic effect with *in vivo* patient responses to therapy.

### Conflict of Interest

The authors do not have conflicting interests to report.

### Acknowledgements

The authors would like to thank Dr. Pramod Garg from the All India Institute of Medical Sciences, New Delhi, India for critically revising the manuscript.

M.P. Peppelenbosch is supported by NWO-ALW (840.12.001) and a personal ECCO grant. H. Braat was supported by a Gastrostart grant from the Dutch Society of the Digestive Diseases.

### Appendix A. Supplementary material

Supplementary data associated with this article can be found, in the online version, at <http://dx.doi.org/10.1016/j.canlet.2014.01.014>.

### References

- [1] A. Jemal, F. Bray, M.M. Center, J. Ferlay, E. Ward, D. Forman, Global cancer statistics, *CA Cancer J. Clin.* 61 (2011) 69–90.
- [2] H. Oettle, S. Post, P. Neuhaus, K. Gellert, J. Langrehr, K. Ridwelski, H. Schramm, J. Fahlke, C. Zuelke, C. Burkart, K. Gutberlet, E. Kettner, H. Schmalenberg, K. Weigang-Koehler, W.O. Bechstein, M. Niedergethmann, I. Schmidt-Wolf, L. Roll, B. Doerken, H. Riess, Adjuvant chemotherapy with gemcitabine vs observation in patients undergoing curative-intent resection of pancreatic cancer: a randomized controlled trial, *JAMA* 297 (2007) 267–277.
- [3] U. Rudloff, A.V. Maker, M.F. Brennan, P.J. Allen, Randomized clinical trials in pancreatic adenocarcinoma, *Surg. Oncol. Clin. N. Am.* 19 (2010) 115–150.
- [4] A.C. Society, American Cancer Society. *Cancer Facts & Figures 2012*, Atlanta, American Cancer Society, 2012.
- [5] T. Conroy, F. Desseigne, M. Ychou, O. Bouche, R. Guimbaud, Y. Becouarn, A. Adenis, J.L. Raoul, S. Gourgou-Bourgade, C. de la Fouchardiere, J. Bennouna, J.B. Bachet, F. Khemissa-Akouz, D. Pere-Verge, C. Delbaldo, E. Assenat, B. Chauffert, P. Michel, C. Montoto-Grillot, M. Ducreux, U. groupe tumeurs digestives of, P. intergroup, FOLFIRINOX versus gemcitabine for metastatic pancreatic cancer, *N. Engl. J. Med.* 364 (2011) 1817–1825.
- [6] H. Braat, M. Bruno, E.J. Kuipers, M.P. Peppelenbosch, Pancreatic cancer: promise for personalised medicine?, *Cancer Lett* 318 (2012) 1–8.
- [7] S. Jones, X. Zhang, D.W. Parsons, J.C. Lin, R.J. Leary, P. Angenendt, P. Mankoo, H. Carter, H. Kamiyama, A. Jimeno, S.M. Hong, B. Fu, M.T. Lin, E.S. Calhoun, M. Kamiyama, K. Walter, T. Nikolskaya, Y. Nikolsky, J. Hartigan, D.R. Smith, M. Hidalgo, S.D. Leach, A.P. Klein, E.M. Jaffe, M. Goggins, A. Maitra, C. Iacobuzio-Donahue, J.R. Eshleman, S.E. Kern, R.H. Hruban, R. Karchin, N. Papadopoulos, G. Parmigiani, B. Vogelstein, V.E. Velculescu, K.W. Kinzler, Core signaling pathways in human pancreatic cancers revealed by global genomic analyses, *Science* 321 (2008) 1801–1806.
- [8] C.M. Ardito, B.M. Gruner, K.K. Takeuchi, C. Lubeseder-Martellato, N. Teichmann, P.K. Mazur, K.E. Delgiorno, E.S. Carpenter, C.J. Halbrook, J.C. Hall, D. Pal, T. Briel, A. Herner, M. Trajkovic-Arsic, B. Sipos, G.Y. Liou, P. Storz, N.R. Murray, D.W. Threadgill, M. Sibilica, M.K. Washington, C.L. Wilson, R.M. Schmid, E.W. Raines, H.C. Crawford, J.T. Sivek, EGF receptor is required for KRAS-induced pancreatic tumorigenesis, *Cancer Cell* 22 (2012) 304–317.
- [9] M. Kanda, H. Matthaei, J. Wu, S.M. Hong, J. Yu, M. Borges, R.H. Hruban, A. Maitra, K. Kinzler, B. Vogelstein, M. Goggins, Presence of somatic mutations in most early-stage pancreatic intraepithelial neoplasia, *Gastroenterology* 142 (2012). 730–733 e739.
- [10] N.T. van Heek, A.K. Meeker, S.E. Kern, C.J. Yeo, K.D. Lillemoe, J.L. Cameron, G.J. Offerhaus, J.L. Hicks, R.E. Wilentz, M.G. Goggins, A.M. De Marzo, R.H. Hruban, A. Maitra, Telomere shortening is nearly universal in pancreatic intraepithelial neoplasia, *Am. J. Pathol.* 161 (2002) 1541–1547.
- [11] A.L. Kennedy, P.D. Adams, J.P. Morton, Ras, PI3K/Akt and senescence: paradoxes provide clues for pancreatic cancer therapy, *Small GTPases* 2 (2011) 264–267.
- [12] J. LoPiccolo, G.M. Blumenthal, W.B. Bernstein, P.A. Dennis, Targeting the PI3K/Akt/mTOR pathway: effective combinations and clinical considerations, *Drug resistance updates: reviews and commentaries in antimicrobial and anticancer chemotherapy* 11 (2008) 32–50.



- [13] I. Hofmann, A. Weiss, G. Elain, M. Schwaederle, D. Sterker, V. Romanet, T. Schmelzle, A. Lai, S.M. Brachmann, M. Bentires-Alj, T.M. Roberts, W.R. Sellers, F. Hofmann, S.M. Maira, K-RAS mutant pancreatic tumors show higher sensitivity to MEK than to PI3K inhibition in vivo, *PLoS ONE* 7 (2012) e44146.
- [14] I. Garrido-Laguna, A.C. Tan, M. Uson, M. Angenendt, W.W. Ma, M.C. Villaroel, M. Zhao, N.V. Rajeshkumar, A. Jimeno, R. Donehower, C. Iacobuzio-Donahue, M. Barrett, M.A. Rudek, B. Rubio-Viqueira, D. Laheru, M. Hidalgo, Integrated preclinical and clinical development of mTOR inhibitors in pancreatic cancer, *Br. J. Cancer* 103 (2010) 649–655.
- [15] Y.Y. Zaytseva, J.D. Valentino, P. Gulhati, B.M. Evers, mTOR inhibitors in cancer therapy, *Cancer Lett.* 319 (2012) 1–7.
- [16] H. Zhou, Y. Luo, S. Huang, Updates of mTOR inhibitors, *Anti-Cancer Agents Med. Chem.* 10 (2010) 571–581.
- [17] M.M. Javle, R.T. Shroff, H. Xiong, G.A. Varadhachary, D. Fogelman, S.A. Reddy, D. Davis, Y. Zhang, R.A. Wolff, J.L. Abbruzzese, Inhibition of the mammalian target of rapamycin (mTOR) in advanced pancreatic cancer: results of two phase II studies, *BMC Cancer* 10 (2010) 368.
- [18] H. Takeuchi, Y. Kondo, K. Fujiwara, T. Kanzawa, H. Aoki, G.B. Mills, S. Kondo, Synergistic augmentation of rapamycin-induced autophagy in malignant glioma cells by phosphatidylinositol 3-kinase/protein kinase B inhibitors, *Cancer Res.* 65 (2005) 3336–3346.
- [19] A.M. Bellizzi, M. Bloomston, X.P. Zhou, O.H. Iwenofu, W.L. Frankel, The mTOR pathway is frequently activated in pancreatic ductal adenocarcinoma and chronic pancreatitis, *Appl. Immunohistochem. Mol. Morphol.* 18 (2010) 442–447.
- [20] D.A. Guertin, D.M. Sabatini, An expanding role for mTOR in cancer, *Trends Mol. Med.* 11 (2005) 353–361.
- [21] D.D. Sarbassov, S.M. Ali, D.H. Kim, D.A. Guertin, R.R. Latek, H. Erdjument-Bromage, P. Tempst, D.M. Sabatini, Rictor, a novel binding partner of mTOR, defines a rapamycin-insensitive and raptor-independent pathway that regulates the cytoskeleton, *Curr. Biol.* 14 (2004) 1296–1302.
- [22] J. Chung, C.J. Kuo, G.R. Crabtree, J. Blenis, Rapamycin-FKBP specifically blocks growth-dependent activation of and signaling by the 70 kd S6 protein kinases, *Cell* 69 (1992) 1227–1236.
- [23] D.D. Sarbassov, S.M. Ali, S. Sengupta, J.H. Sheen, P.P. Hsu, A.F. Bagley, A.L. Markhard, D.M. Sabatini, Prolonged rapamycin treatment inhibits mTORC2 assembly and Akt/PKB, *Mol. Cell* 22 (2006) 159–168.
- [24] B.M. Wolpin, A.F. Hezel, T. Abrams, L.S. Blaszkowsky, J.A. Meyerhardt, J.A. Chan, P.C. Enzinger, B. Allen, J.W. Clark, D.P. Ryan, C.S. Fuchs, Oral mTOR inhibitor everolimus in patients with gemcitabine-refractory metastatic pancreatic cancer, *J. Clin. Oncol.* 27 (2009) 193–198.
- [25] Y. Li, J. Deuring, M.P. Peppelenbosch, E.J. Kuipers, C. de Haar, C.J. van der Woude, IL-6-induced DNMT1 activity mediates SOCS3 promoter hypermethylation in ulcerative colitis-related colorectal cancer, *Carcinogenesis* 33 (2012) 1889–1896.
- [26] J.L. Hornick, G.Y. Lauwers, R.D. Odze, Immunohistochemistry can help distinguish metastatic pancreatic adenocarcinomas from bile duct adenomas and hamartomas of the liver, *Am. J. Surg. Pathol.* 29 (2005) 381–389.
- [27] E. Missiaglia, I. Dalai, S. Barbi, S. Beghelli, M. Falconi, M. della Peruta, L. Piemonti, G. Capurso, A. Di Florio, G. delle Fave, P. Pederzoli, C.M. Croce, A. Scarpa, Pancreatic endocrine tumors: expression profiling evidences a role for AKT-mTOR pathway, *J. Clin. Oncol.* 28 (2010) 245–255.
- [28] A. Efeyan, D.M. Sabatini, mTOR and cancer: many loops in one pathway, *Curr. Opin. Cell Biol.* 22 (2010) 169–176.
- [29] K. Yu, L. Toral-Barza, C. Shi, W.G. Zhang, J. Lucas, B. Shor, J. Kim, J. Verheijen, K. Curran, D.J. Malwitz, D.C. Cole, J. Ellingboe, S. Ayril-Kaloustian, T.S. Mansour, J.J. Gibbons, R.T. Abraham, P. Nowak, A. Zask, Biochemical, cellular, and in vivo activity of novel ATP-competitive and selective inhibitors of the mammalian target of rapamycin, *Cancer Res.* 69 (2009) 6232–6240.
- [30] G. Garcia-Echeverria, Blocking the mTOR pathway: a drug discovery perspective, *Biochem. Soc. Trans.* 39 (2011) 451–455.
- [31] A. Britschgi, R. Andraos, H. Brinkhaus, I. Klebba, V. Romanet, U. Muller, M. Murakami, T. Radimerski, M. Bentires-Alj, JAK2/STAT5 inhibition circumvents resistance to PI3K/mTOR blockade: a rationale for cotargeting these pathways in metastatic breast cancer, *Cancer Cell* 22 (2012) 796–811.
- [32] P.J. Fitzgerald, Homogeneity and heterogeneity in pancreas cancer: presence of predominant and minor morphological types and implications, *Int. J. Pancreatol.* 1 (1986) 91–94.
- [33] J.L. Kopp, G. von Figura, E. Mayes, F.F. Liu, C.L. Dubois, J.P. Morris, F.C. Pan, H. Akiyama, C.V. Wright, K. Jensen, M. Hebrok, M. Sander, Identification of Sox9-dependent acinar-to-ductal reprogramming as the principal mechanism for initiation of pancreatic ductal adenocarcinoma, *Cancer Cell* 22 (2012) 737–750.
- [34] Z.J. Dai, J. Gao, X.B. Ma, H.F. Kang, B.F. Wang, W.F. Lu, S. Lin, X.J. Wang, W.Y. Wu, Antitumor effects of rapamycin in pancreatic cancer cells by inducing apoptosis and autophagy, *Int. J. Mol. Sci.* 14 (2012) 273–285.
- [35] A. Iwamaru, Y. Kondo, E. Iwado, H. Aoki, K. Fujiwara, T. Yokoyama, G.B. Mills, S. Kondo, Silencing mammalian target of rapamycin signaling by small interfering RNA enhances rapamycin-induced autophagy in malignant glioma cells, *Oncogene* 26 (2007) 1840–1851.
- [36] S. Yang, X. Wang, G. Contino, M. Liesa, E. Sahin, H. Ying, A. Bause, Y. Li, J.M. Stommel, G. Dell'antonio, J. Mautner, G. Tonon, M. Haigis, O.S. Shirihai, C. Doglioni, N. Bardeesy, A.C. Kimmelman, Pancreatic cancers require autophagy for tumor growth, *Genes Dev.* 25 (2011) 717–729.
- [37] W. van Veele, S.E. Korsse, L. van de Laar, M.P. Peppelenbosch, The long and winding road to rational treatment of cancer associated with LKB1/AMPK/TSC/mTORC1 signaling, *Oncogene* 30 (2011) 2289–2303.
- [38] E. Avizienyte, A. Loukola, S. Roth, A. Hemminki, M. Tarkkanen, R. Salovaara, J. Arola, R. Butzow, K. Husgafvel-Pursiainen, A. Kakkola, H. Jarvinen, L.A. Aaltonen, LKB1 somatic mutations in sporadic tumors, *Am. J. Pathol.* 154 (1999) 677–681.
- [39] G.H. Su, R.H. Hruban, R.K. Bansal, G.S. Bova, D.J. Tang, M.C. Shekher, A.M. Westerman, M.M. Entius, M. Goggins, C.J. Yeo, S.E. Kern, Germline and somatic mutations of the STK11/LKB1 Peutz-Jeghers gene in pancreatic and biliary cancers, *Am. J. Pathol.* 154 (1999) 1835–1840.
- [40] H.J. Klumpen, K.C. Queiroz, C.A. Speck, C.J. van Noesel, H.C. Brink, W.W. de Leng, R.F. de Wilde, E.M. Mathus-Vliegen, G.J. Offerhaus, M.A. Alleman, A.M. Westermann, D.J. Richel, mTOR inhibitor treatment of pancreatic cancer in a patient with Peutz-Jeghers syndrome, *J. Clin. Oncol.* 29 (2011) e150–e153.
- [41] T. Asano, Y. Yao, J. Zhu, D. Li, J.L. Abbruzzese, S.A. Reddy, The PI 3-kinase/Akt signaling pathway is activated due to aberrant Pten expression and targets transcription factors NF-kappaB and c-Myc in pancreatic cancer cells, *Oncogene* 23 (2004) 8571–8580.
- [42] J.C. Yao, M.H. Shah, T. Ito, C.L. Bohas, E.M. Wolin, E. Van Cutsem, T.J. Hobday, T. Okusaka, J. Capdevila, E.G. de Vries, P. Tomassetti, M.E. Pavel, S. Hoosen, T. Haas, J. Lincy, D. Leibold, K. Oberg, T.T.S.G. Rad001 in advanced neuroendocrine tumors, everolimus for advanced pancreatic neuroendocrine tumors, *N. Engl. J. Med.* 364 (2011) 514–523.
- [43] J. Baselga, M. Campone, M. Piccart, H.A. Burris 3rd, H.S. Rugo, T. Sahnoud, S. Noguchi, M. Gnani, K.I. Pritchard, F. Lebrun, J.T. Beck, Y. Ito, D. Yardley, I. Deleu, A. Perez, T. Bachelot, L. Vittori, Z. Xu, P. Mukhopadhyay, D. Leibold, G.N. Hortobagyi, Everolimus in postmenopausal hormone-receptor-positive advanced breast cancer, *N. Engl. J. Med.* 366 (2012) 520–529.
- [44] R.J. Motzer, B. Escudier, S. Oudard, T.E. Hutson, C. Porta, S. Bracarda, V. Grunwald, J.A. Thompson, R.A. Figlin, N. Hollaender, G. Urbanowitz, W.J. Berg, A. Kay, D. Leibold, A. Ravaud, R.-S. Group, Efficacy of everolimus in advanced renal cell carcinoma: a double-blind, randomised, placebo-controlled phase III trial, *Lancet* 372 (2008) 449–456.
- [45] G. von Wichert, P.M. Jehle, A. Hoeflich, S. Koschnick, H. Dralle, E. Wolf, B. Wiedenmann, B.O. Boehm, G. Adler, T. Seufferlein, Insulin-like growth factor-I is an autocrine regulator of chromogranin A secretion and growth in human neuroendocrine tumor cells, *Cancer Res.* 60 (2000) 4573–4581.